Construction and Building Materials 401 (2023) 132978

Contents lists available at ScienceDirect

Construction and Building Materials

journal homepage: www.elsevier.com/locate/conbuildmat

Evaluation of the optimal concrete mix design with coconut shell ash as a partial cement replacement

Kavishan Sathsara Ranatunga [a,*,1], Enrique del Rey Castillo [b], Charlotte Louise Toma [b]

[a] Department of Civil Engineering, Surveying and Construction Management, Kingston University London, Kingston upon Thames, Surrey, United Kingdom
[b] Department of Civil and Environmental Engineering, University of Auckland, Symonds Street, Auckland 1010, New Zealand

ARTICLE INFO

Keywords:
Sustainability
Sustainable concrete
SCMs
Optimal concrete mix
Life cycle assessment

ABSTRACT

Concrete is a major construction material with a significant environmental impact. Among other materials, coconut shell ash could be used as a partial replacement of cement to produce sustainable concrete. This study aimed to investigate the use of coconut shell ash as a partial cement replacement to reduce the environmental impact whilst achieving the predefined structural performance of concrete. The fresh, hardened and micro-structural properties were investigated, and a life cycle assessment within the product stage was conducted in this study. When considering 15%, 20%, 25% and 30% replacement level concrete mixes, compressive strength was 27.31 MPa, 26.94 MPa, 25.60 MPa and 21.40 MPa at 28 days and environmental impact reduction in global warming potential were over 10%, 15%, 20% and 25% respectively. Based on the structural performance and environmental impact, 20% was the optimal replacement level. Therefore, cement can be replaced by coconut shell ash up to 20% to achieve the average target compressive strength as 25 MPa by reducing the environmental impact in global warming potential over 15%.

1. Introduction

1.1. Background

Concrete is a widely used material for a range of applications, such as buildings, bridges, roads, dams, and many other types of infrastructure, which makes concrete the second most commonly used material in the world after water [55]. Cement is the governing contributor to greenhouse gas emissions and is responsible for over 7% of greenhouse gas emissions [40], although cement is only a small fraction (typically 10% − 15% by volume) [44]. Cement manufacturing uses significant raw materials, mainly limestone and clay, calcinating them at a temperature between 1,400 °C and 1,600 °C to reactivate and produce clinker, releasing a significant amount of greenhouse gases [4]. Greenhouse gases are emitted from three sources: 1) excavation of raw materials using machinery that burns fossil fuels, 2) calcinating the raw materials, where fossil fuels are also burned, and 3) through the chemical processes of producing cement. Therefore, cement production for construction plays a significant role in global warming, primarily driven by humans [29].

The large consumption of cement and the extensive release of greenhouse gases during its production requires alternative binding materials to reduce the environmental impact of concrete used in the construction industry. These alternative binding materials are generally called supplementary cementitious materials (SCMs) and they are added to concrete mixture as a part of the total cementitious system to improve the properties of concrete such as workability, density, compressive strength and durability, and to reduce the negative impacts on the environment. Supplementary cementitious materials can contribute to concrete quality through hydraulic activity, pozzolanic activity, or both [35]. SCMs with hydraulic activity can harden through the reaction with water by forming calcium-silicate-hydrate gel – commonly known as C-S-H gel. SCMs that have pozzolanic activity can harden through the reaction with water and calcium hydroxide [52].

Today commonly used supplementary cementitious materials are fly ash, silica fume, slag and metakaolin [4]. Fly ash is a fine by-product resulting from the burning of coal at high temperatures in electric power generating [4]. Particle size and chemical composition of the fly ash affects to performance of concrete [21,24]. A large number of studies have been published on the performance of concrete with fly ash [43,59,58,32,2]. Silica fume is also a commonly used supplementary cementitious material in the industry. Silica fume is an industrial by-

* Corresponding author.
E-mail addresses: kran503@aucklanduni.ac.nz (K.S. Ranatunga), e.delrey@auckland.ac.nz (E. del Rey Castillo), charlotte.toma@auckland.ac.nz (C.L. Toma).
[1] Presnt address: Department of Civil and Environmental Engineering, University of Auckland, Symonds Street, Auckland 1010, New Zealand.

https://doi.org/10.1016/j.conbuildmat.2023.132978
Received 10 May 2023; Received in revised form 5 August 2023; Accepted 12 August 2023
Available online 17 August 2023

product of the production of silicon metals and ferrosilicon alloys in electric-arc furnaces [35]. Silica fume has high pozzolanic activity due to its small particle size and chemical composition [4]. Silica fume can improve the pore structure in two ways to increase the durability and the compressive strength of concrete. One way is that silica fume has a filler effect by filling the paste's gaps between cement grains or paste's gaps between cement grains and aggregates. Other way is that silica fume reacts with calcium hydroxide is to produce a greater solid volume of C-S-H gel [11]. Concrete with silica fume as a SCM shows higher compressive strength after 56 days despite delaying the strength gain [3,33]. Slag is a by-product of the metallurgy industry. It is used as a supplementary cementitious material because of both hydraulic and pozzolanic activity [35]. The compressive strength of concrete increases up to the optimal level with increasing slag cement content but it is reducing the early strength of concrete [42]. Metakaolin is also a supplementary cementitious material but not an industrial by-product. Metakaolin is produced by calcinating kaolin clay at a temperature ranging between 650 °C and 800 °C [35]. It increases the compressive strength and durability of concrete through the pozzolanic activity [48]. Many studies have been performed with metakaolin to determine the concrete properties and it is a excellent material to replace the cement [9,46,47,60].

The construction industry faces traditional supplementary cementitious materials shortage for various reasons. Most countries including the US, UK and Netherlands are planning to retire coal-fired power plants because of air pollution and it affects for the fly ash supply [31]. Furthermore, annual global cement production has reached 5.17 billion tons in 2020 and the cement market is expected to grow by 3.3% annually in the forecast period of 2023–2028 [26]. Therefore, developing alternative cementitious materials has become a critical requirement globally to maintain the supply chain of supplementary cementitious materials.

Coconut is an important crop in many tropical countries, but large quantities of coconut shells are currently disposed of in landfills due to the higher demand of coconut based products. Fifty billion coconuts are grown yearly, and 85% of coconut shells are treated as waste worldwide [41]. Standard landfilling processes produce greenhouse gases, mainly methane, when coconut shells are decomposed as organic materials [39] in addition to increasing water pollution and soil pollution. Reusing coconut shells to eliminate the environmental pollution from landfilling is a high priority for developing countries in the tropical zone such as Sri Lanka.

Coconut shell ash (CSA) is produced by burning coconut shells. It commonly has black colour because of the high amount of unburned carbon [23]. In previous studies, coconut shells were burned for 4 to 6 h to produce CSA [1,57,12]. The coconut shell ash's physical and chemical properties depend on the source and the production process. Suitable processing techniques can improve both physical and chemical properties such as particle size, particle shape and reactive oxides involved for pozzolanic reaction. Some chemical constituents in the CSA, such as lime (CaO), silica (SiO_2), alumina (Al_2O_3), and iron oxide (Fe_2O_3), are the same as the chemical constituents in cement [37], suggesting that CSA can provide cementitious properties if used as a SCM in concrete. A high amount of reactive silica (SiO_2) in the CSA reacts with water and calcium hydroxide to form C-S-H gel in concrete [23].

Some studies have been conducted to investigate the properties of concrete with CSA as a supplementary cementitious material, but without properly studying the environmental impact. Workability is a commonly investigated property of fresh concrete, typically measured by the slump cone test as per the BS EN 12350-2:2019 [17]. Previous studies have reported that the workability of concrete reduces with increasing CSA content based on its irregular shape, higher surface area, and carbon particles [23]. Therefore, water demand increases with increasing CSA content to achieve the desired slump value [12]. According to these studies, the slump of concrete can be increased through the coconut shell ash's grinding process.

Density is a property of concrete measured according to the BS EN 12390-7:2019 [20]. Previous studies have shown that concrete density can be reduced by increasing the CSA content to the maximum replacement level [56,12]. Concrete density contributes to the dead load of concrete structures, and therefore past researchers have focused on the density of concrete when selecting the optimal replacement level.

Compressive strength is usually the most critical parameter of concrete. When CSA is added to concrete as a supplementary cementitious material, the compressive strength increases up to an optimal replacement level, decreasing beyond that optimal replacement level [23]. This phenomenon is attributed to the pore filling effect and the pozzolanic reaction of the CSA. Beyond the optimal percentage, the pore filling effect and pozzolanic reaction reduce due to the dilution effect of cement. The dilution effect means existing cement content is low due to the higher CSA content, and therefore produced calcium hydroxide- resulting from the hydration of Portland cement- is also low. In the previous studies, CSA has been substituted for cement by focusing on various target compressive strengths of concrete after 28 days of curing. Previous studies have focused on maximum cement replacement levels of 20%, 25% and 30%. In every study, the maximum compressive strength was observed for the 10% replacement mix, and the mixes at higher replacement levels showed less compressive strength than the control mix at the age of 28 days [36,57,12]. Some studies have observed that compressive strength at 28 days of the control mix and the 10% replacement mix are similar, and compressive strength decreases with increasing the CSA content [56,1]. Previous studies have found that CSA significantly impacts hardened concrete properties. However, no optimal concrete mix design was obtained beyond the 10% replacement level with CSA burned for more than 4 h.

The performance of concrete with CSA has not been studied in Sri Lanka, even though many coconut shells are disposed of in landfills. In previously published research, coconut shells were burned for more than 4 h to minimize the higher carbon content and increase the percentage of silica content, which contributes to form C-S-H gel. In this study, coconut shells were burned only for 2 h to minimize the environmental impact because burning coconut shells contributes for carbon dioxide emission due to the usage of energy and changing chemical composition. Any study was not conducted to determine an optimal replacement level based on both the structural performance and environmental impact using CSA by limiting the burning to only for 2 h.

The aim of this research was to investigate the optimal concrete mix design of concrete with CSA as a supplementary cementitious material to reduce the environmental impact described in BS EN 15804:2012+A1:2013 [14] whilst achieving defined structural performance. The target compressive strength of concrete after 28 days of curing was 25 MPa in this study. Previously published research has not focused on the 25 Mpa as the target compressive strength of concrete with CSA by limiting the burning only for 2 h. Developing a concrete mix to obtain the target compressive strength of 25 MPa is critical because structural designs are commonly carried out with a target compressive strength of 25 MPa in Sri Lanka [51].

The objective of this research was to identify the physical, chemical and microstructural properties of concrete mixes with CSA as a cement replacement, and most importantly properly quantify the environmental impacts. Coconut shells were burned under controlled conditions to remove the carbon, but the burning was limited to 2 h to reduce the environmental impact. The mix design was carried out according to the Building Research Establishment (BRE) method [53]; therefore, concrete industry can easily follow the proposed mix design in future.

2. Materials and methodology

2.1. Materials

The following materials were used in this research.

2.1.1. *Ordinary Portland cement*

Ordinary Portland cement with strength class 42.5 N was used for this research. Scanning electron microscopy (SEM) analysis, X-ray fluorescence (XRF) analysis, energy dispersive spectroscopy (EDS) analysis, and dynamic image (DIA) analysis were performed to determine the properties of cement as discussed in Section 2.2.2.

2.1.2. *Coconut shell ash*

This research has used CSA as the supplementary cementitious material. It was produced by burning, grinding and sieving processes, and more details on the manufacturing process are included in Section 2.2.1 below. SEM, EDS, XRF, and DIA analyses were performed to determine the properties of the CSA and to compare it with cement, as discussed in section 2.2.2.

2.1.3. *Water*

Tap water was used for this study with drinking quality and was free from organic matters.

2.1.4. *Fine aggregate*

Clean river sand was used as fine aggregate to produce concrete. The sieve analysis test was performed according to the BS EN 933-2:2020 [19] to determine the particle size distribution curve, as shown in Fig. 1. The upper limit was 5 mm and the lower limit was 0.15 mm. The specific gravity of the fine aggregate was 2.62, and water absorption was 0.93% as per the specific gravity and the water absorption test, which was performed according to the BS EN 1097-6:2013 [16].

2.1.5. *Coarse aggregate*

Crushed stones less than 20 mm were used as coarse aggregate to produce concrete. The sieve analysis test was performed according to the BS EN 933-2:2020 [19] to determine the particle size distribution curve, as shown in Fig. 1. The upper limit was 20 mm and lower limit was 5 mm. The specific gravity of the coarse aggregate was 2.81, and water absorption was 0.62% as per the specific gravity and the water absorption test, which was performed according to the BS EN 1097-6:2013 [16].

2.2. *Experimental procedure*

The experimental process was divided into four parts. Firstly, CSA was prepared. Secondly, the properties of materials were determined through numerous tests. Then concrete with CSA was developed to achieve the target compressive strength after 28 days of curing as 25 MPa as the third step. Finally, the properties of concrete were investigated by performing various tests to determine the most optimal concrete mix design.

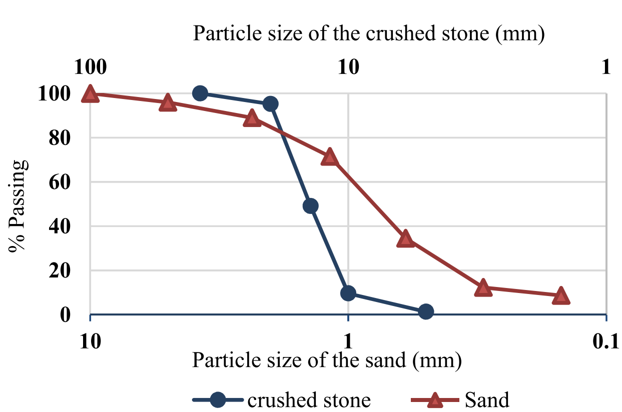

Fig. 1. Particle size distribution curve of fine and coarse aggregate.

2.2.1. *Preparation of coconut shell ash*

Newly removed coconut shells as domestic waste were used for this study to produce the CSA. Coconut shells were cleaned and dried under the sun for 6 h to remove moisture.

Then coconut shells were burned at a temperature of 800 °C for 2 h with a diesel incinerator, limiting the burning time to reduce the negative impact on the environment. The weight of the coconut shells reduced up to 39.3% after the burning.

Then the sample was milled with a grinding machine into smaller particles. The milling process was performed for 5 min for each Kg of CSA. Then the sample was sieved using a 75 μm sieve. Fig. 2 shows the formation of CSA from the coconut shells.

2.2.2. *Determination of the material properties*

The particle shapes of the cement and CSA were observed through the SEM analysis according to the ASTM C1723-16 [8] using a ZEISS EVO 18 machine. DIA analysis was performed using the Camsizer X2 instrument to identify the properties of cement and CSA particles: shape and size. In addition, the particle size distribution curves of the cement and CSA also were observed by DIA analysis. When water is added to concrete, cement reacts with water to harden. Therefore, the determination of chemical composition was essential, and XRF analysis was performed to determine the chemical composition of cement and CSA. Fischer XAN-FD machine was used to perform the XRF analysis according to the ASTM E1621 [7]. In this research, XRF analysis did not indicate all existing cement and CSA elements. It was difficult to determine the light elements because they have low energy levels [34]. Therefore, EDS analysis with the SEM was performed to determine the chemical composition of cement and CSA with higher precision and sensitivity. Sieve analysis, moisture content, and specific gravity and water absorption tests were conducted for the coarse and fine aggregate according to the standards to find the parameters used for the mix design calculation.

2.2.3. *Development of concrete with coconut shell ash*

Concrete mix design without CSA was initially observed according to the Building Research Establishment (BRE) method [53] to achieve the target compressive strength as 25 Mpa after 28 days of curing. In the design, water to cement binder ratio was selected as 0.55. Then cement was replaced with CSA in different percentages to determine concrete properties according to Table 1. Concrete mixes were named as CSA 0, CSA 15, CSA 20, CSA 25, and CSA 30 when CSA replaced the cement by 0%, 15%, 20%, 25% and 30% respectively. This research was conducted to mitigate the environmental impact of concrete production whilst achieving defined structural performance. The production process of the

Fig. 2. Formation of coconut shell ash from the coconut shells.

Table 1
Mix proportions of materials in concrete.

Mix ID	Cement (kg/m^3)	CSA (Kg/m^3)	Fine aggregate-SSD (kg/m^3)	Coarse aggregate-SSD (kg/m^3)	Water (L)
CSA 0	372.7	0	867.5	939.8	205
CSA 15	316.8	55.9	867.5	939.8	205
CSA 20	298.2	74.5	867.5	939.8	205
CSA 25	279.5	93.2	867.5	939.8	205
CSA 30	260.9	111.8	867.5	939.8	205

CSA was also different from the previous research studies. Therefore cement was replaced with CSA in 15% weight as the first replacement to decide whether to select higher or lower percentages. Based on the target compressive strength of the CSA 15 mix, cement was replaced in higher percentages with CSA. Nine cubes were cast for every concrete mix, three cubes for each 7 days, 28 days, and 56 days.

2.2.4. Determination of the properties of concrete with coconut shell ash

Various tests were performed to determine the fresh, hardened, and microstructural properties of concrete. Slump and temperature were determined as fresh concrete properties at the casting time of every mix. Then three cubes were tested at 7 days, 28 days, and 56 days of curing period for every mix to determine the hardened concrete properties – compressive strength, density and water absorption – and microstructural properties of concrete were investigated using SEM images. The properties of concrete were measured at 56 days because pozzolanic reactions take a long period to occur than hydraulic reactions.

3. Results and discussion

This section presents the results of this research and discusses concrete performance and the optimal concrete mix designs.

3.1. Properties of cement and coconut shell ash

The physical, chemical and microstructural properties of the cement and CSA were initially tested to identify the effect on concrete performance.

3.1.1. Physical properties of cement and coconut shell ash

Dynamic image analysis was conducted to determine the physical characteristics of the cement and CSA particles according to the ISO 13322-2: 2006 [30]. Fig. 3 shows the particle size-frequency distribution curves with the particle percentage (%) against the particle size. In addition, the properties of the cement and CSA particles are shown in

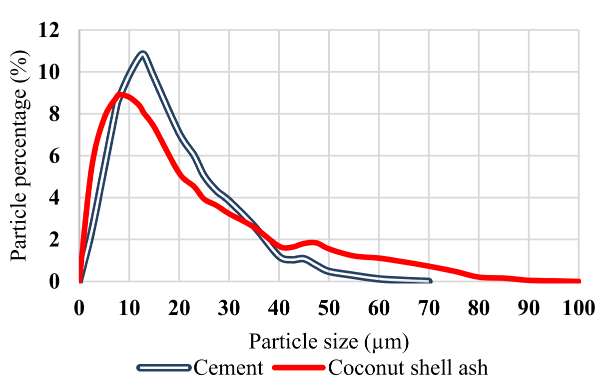

Fig. 3. Particle size-frequency distribution curves of cement and CSA.

Table 2
Physical properties of cement and CSA.

Property	Cement	CSA
Diameter of the particle corresponding to 90% finer	34.3 μm	55.9 μm
Diameter of the particle corresponding to 50% finer	16.5 μm	16.9 μm
Diameter of the particle corresponding to 10% finer	7.1 μm	4.3 μm
Portion of the particles smaller than 45.5 μm	97.3 %	84.0 %
Sphericity of the particles	0.79	0.83
Symmetry of the particles	0.87	0.89

Table 2. The size and shape/sphericity of the cement and CSA particles affects hydration, strength development, workability, and other properties of concrete [61].

After grinding, CSA was sieved using a 75 μm sieve to obtain fine particles to replace the cement. Unexpectedly, the size of some sieved CSA particles was more than 75 μm even though it was sieved through the 75 μm sieve, which suggests that not all ash particles were spherical. This hypothesis was proved by the sphericity of CSA particles (0.83) in Table 2 and by the microstructural image of the CSA particles described in Section 3.1.3. The sphericity of the CSA particles (0.83) is more than the sphericity of the cement particles (0.79), as shown in Table 2. Spherical particles contribute for increasing the workability of concrete because of the lubrication effect. Therefore, CSA can increase the workability of concrete based on the sphericity.

As per Fig. 3, the size of the CSA particles has varied from 0 μm to 100 μm, and the size of the cement particles has varied from 0 μm to 70 μm due to the different crushing ways of the grinding machine and the cement mill. Most of the cement and CSA particles are between the 8.9 μm and 35.4 μm size range, and more cement particles than CSA particles are present in this size range. According to Fig. 3, CSA has more coarse particles above 35.4 μm in size than cement. Table 2 also presents that 10% of total cement particles were larger than 34.3 μm, and 10% of total CSA particles were larger than 55.9 μm. These findings indicate that CSA has more coarse particles than cement. According to Fig. 3, CSA has more fine particles below 8.9 μm in size than cement. Table 2 also presents that 10% of cement particles were smaller than 7.1 μm and 10% of CSA particles were smaller than 4.3 μm. These findings indicate that CSA has more fine particles than cement. Overall, CSA higher amount of coarse particles and little amount of fine particles, according to Fig. 3. The coarse particles were formed due to insufficient grinding and a higher amount of carbon. Therefore, CSA can increase the workability of concrete and decrease the reactivity during hydration because of less surface area. However, due to the higher amount of carbon particles, CSA can contribute for decreasing the workability of concrete.

Typically, cement is produced with excellent gradation to prevent the voids in the cement paste. According to Fig. 3, CSA has a better gradation than cement to give a better filler effect in concrete than cement. Therefore, CSA may increase the strength of concrete based on the particles properties alone.

3.1.2. Chemical properties of cement and coconut shell ash

XRF analysis and EDS analysis were performed to determine the

Table 3
Chemical composition of cement and coconut shell ash.

	XRF analysis		EDS analysis	
Element	Norm. Wt. (%) in cement	Norm. Wt. (%) in CSA	Norm. Wt. (%) in cement	Norm. Wt. (%) in CSA
Ca	90.85	10.59	39.16	–
Si	–	–	6.94	0.55
Fe	8.71	52.19	6.67	–
Al	–	–	3.78	–
Mg	–	–	1.14	–
K	–	27.88	–	1.93
C	–	–	2.19	87.52
Mn	–	4.36	–	–

chemical composition of the cement and CSA shown in Table 3. XRF analysis and EDS analysis were conducted as per the ASTM E1621 [7] and ASTM E1508-12a [6], respectively. Both analyses have considered the sum of the identified elements' weight as total weight. Therefore, both XRF analysis and EDS analysis are not perfectly accurate. XRF and EDS have not shown the same results because of different reasons: 1). XRF uses an X-ray beam and EDS uses an electron beam to produce characteristic X-rays to evaluate the chemical composition, and 2). EDS instrument had a vacuum chamber, but XRF instrument did not. The lack of vacuum chamber in the XRF instrument mad it difficult for characteristic X-ray of light elements to reach the detector. Additionally, EDS is more surface sensitive than XRF. In this study, the combination of XRF and EDS allowed to identify the elements accurately and confidentially.

Cement consists of CaO, SiO_2, Fe_2O_3, Al_2O_3 and MgO, and CSA consists of CaO, SiO_2, Fe_2O_3, K_2O and Mn_2O_3, according to Table 3. XRF analysis and EDS analysis have not been able to show the amount of Al_2O_3 in CSA even if it exists as per the previous studies [1,57]. The reason for this inconsistency is the small amount of Al_2O_3 present in the CSA and its lightness, making it difficult for the instrument to detect. Additionally, characteristics X-rays are sometimes reabsorbed by the sample or blocked by the air between the sample and detector, escaping detection by the instruments [10,45].

Both XRF and EDS analyses have indicated the presence of K2O in the coconut shell ashCSA, an alkali metal oxide that increases the early strength at the cost of reducing the strength at later stages [4]. The presence of Mn_2O_3 in the CSA has been only determined by XRF analysis and only in a small amount. Therefore, it can be assumed that Mn_2O_3 has little effect on concrete [4]. Typically, MgO in the cement can cause cracking and strength losses due to internal expansion. According to Table 3, the MgO content in the CSA was lower than in cement, or maybe even there was no MgO in the CSA. Therefore, CSA can reduce the negative impact given by the existing MgO of the cement on concrete.

Generally speaking, CaO and SiO_2 are involved in forming C-S-H gel, and Fe_2O_3 and Al_2O_3 contribute to producing C-A-S-H gel and C-A-H gel. EDS analysis has indicated that CSA consists of more carbon than cement because the burning of coconut shells was limited to 2 h. Carbon particles can absorb free water in concrete. Therefore, CSA can reduce the workability of concrete by limiting the free water content. SiO_2 in supplementary cementitious materials typically reacts with water in the presence of $Ca(OH)_2$ to form C-S-H gel. Therefore, these supplementary cementitious materials are considered as pozzolans (American Concrete [4]. CSA can be considered as a pozzolan because it has SiO_2, and it reacts with water in the presence of $Ca(OH)_2$ only [23]. According to Table 3, CSA consists of less SiO_2 than cement. Therefore, it gives a minimal contribution for forming C-S-H gel compared to cement, and it seems CSA can reduce the strength of concrete. Typically $Ca(OH)_2$ increases the macroporosity of the cement paste in concrete [22]. However, the formation of $Ca(OH)_2$ by CSA can be negligible because of the small amount of CaO as per Table 3. Furthermore, CSA helps reduce the macroporosity of concrete through the pozzolanic reaction with $Ca(OH)_2$ formed by cement hydration.

3.1.3. Microstructural properties of cement and coconut shell ash

Examination of microstructural properties of the cement and CSA is critical to understand how CSA changes concrete behaviour. SEM tests were performed to observe the surface SEM images of cement and CSA according to the ASTM C1723-16 [8]. Fig. 4 displays that coconut shell has more fine particles below 8.9 μm in size and more coarse particles above 35.4 μm in size than cement. Cement has more particles than CSA between the 8.9 μm and 35.4 μm size range. Therefore, SEM images illustrated similar results given by the DIA analysis. SEM images indicate that not all cement and CSA particles were spherical, as corroborated by the DIA analysis. However, it is difficult to compare the overall sphericity between cement and CSA based on the SEM images.

As shown in Fig. 4, CSA has given a denser SEM image than cement because small particles fill the voids between larger particles. It is clear that CSA has a better filler effect than cement, similar to other supplementary cementitious materials [11]. Considering the surface of the cement and CSA particles at higher magnification, it seems the surface of the CSA particles is a little bit rougher than the surface of cement particles. The phenomenon is due to the grinding method - CSA particles were ground using a grinding machine, and cement particles were ground using a cement mill. Therefore, CSA can reduce the workability of concrete than cement.

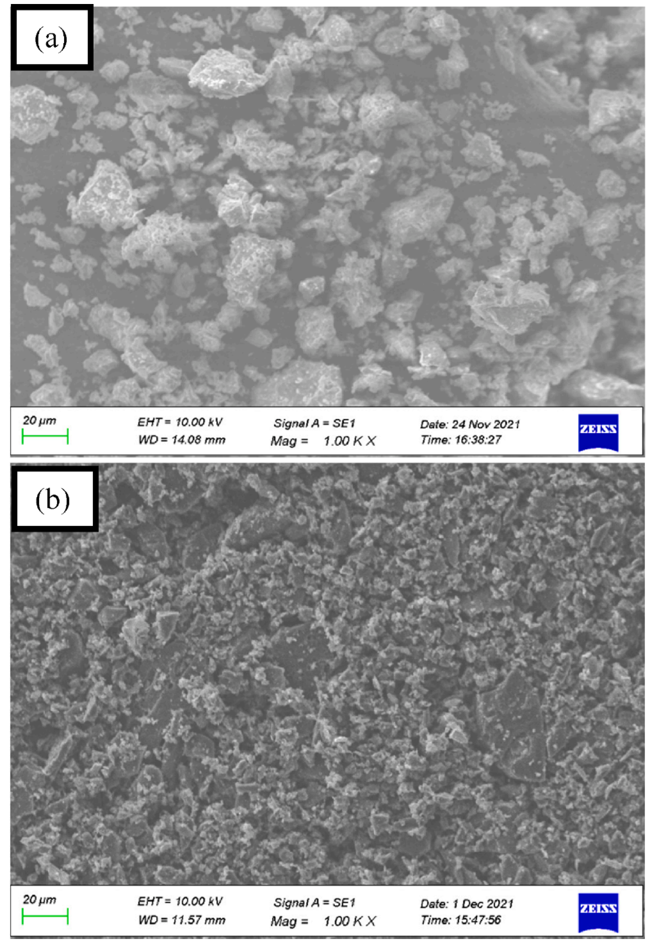

Fig. 4. Surface SEM images of (a) cement, (b) CSA.

3.2. Properties of fresh concrete

In this research, fresh concrete properties were determined to identify the effect of the CSA when replacing the cement. This section presents and discusses the fresh concrete properties: workability and temperature.

3.2.1. Slump

Slump typically indicates the workability of the fresh concrete. The slump of all concrete mixes was determined according to BS EN 12350–2:2019 [17] by doing the slump cone test. Fig. 5 shows the variation of the slump of concrete mixes at 0 h, 0.5 h and 1 h after the mixing. The slump of concrete decreased with increasing the CSA content, from 140 mm in the control mix (CSA 0) to 20 mm in the 30% cement replacement mix (CSA 30). The slump was selected between 60 mm and 180 mm in the design according to the BRE method, so the slump of 140 mm indicated that the selected mix design is correct. In this research, the water to binder (w/b) ratio for every concrete mix was maintained at 0.55 without admixtures and without considering the

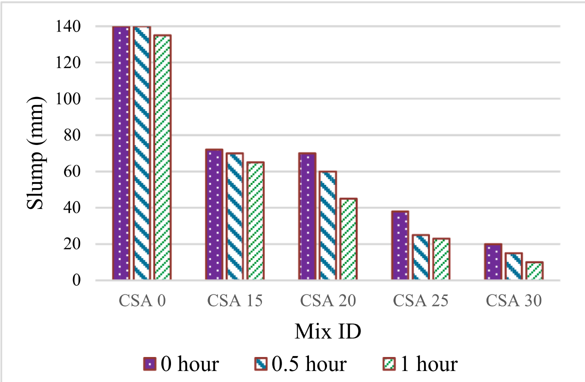

Fig. 5. Variation of the slump after mixing.

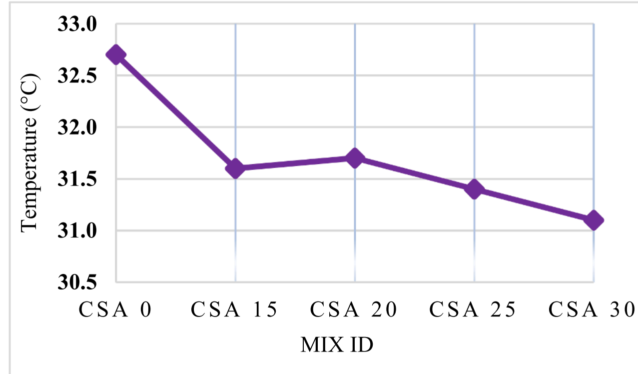

Fig. 6. Temperature of mixes at the time of mixing.

water absorption of CSA. The reduction in workability was more pronounced with a slight increase in CSA, and the 15% replacement level (CSA 15) already reduced the slump by 48.6%. The slump further reduced by 50%, 72.9% and 85.7% for the CSA 20, CSA 25 and CSA 30 mixes at the time of mixing. In addition, within the 0.5 h after mixing, the slump of concrete mixes of CSA 15, CSA 20, CSA 25 and CSA 30 reduced even though the CSA 0 had a constant slump, as shown in Fig. 5.

As explained in Section 3.1, some properties of CSA can increase the workability, while other properties can reduce the workability of concrete. However, it seems that CSA contributed for reducing the slump of concrete when w/b ratio was constant. Two reasons caused the reduction of workability. The first reason was the presence of carbon particles. As per the physical and chemical properties, CSA consisted of higher carbon content than cement. Carbon particles absorb more water from concrete mixes and reduce the free water content. Therefore, slump of concrete mixes reduced due to the insufficient lubrication effect in the cement paste. As shown in Fig. 5, the slump decreased with increasing the CSA content because of decreasing free water content in concrete mixes, and that was consistent with previous studies [23]. In addition, carbon articles have contributed to absorb existing free water quickly within 0.5 h after mixing, as illustrated in Fig. 5. The second reason was the surface roughness of CSA. As per the microstructural properties, CSA particles' surface was rougher than the cement particles' surface. A rough surface provides a more limited lubricant effect than a smooth surface. Therefore, the slump of concrete mixes reduced with increasing the CSA content, as shown in Fig. 5, due to the increasing overall roughness.

When slump is less than 40 mm, concrete mixes are used for the foundation with light reinforcement. But for the normal reinforcement concrete mixes, slump should be more than 40 mm [38]. In this research, CSA 15 and CSA 20 mixes are the best mixes based on the slump because their slump is more than 40 mm. However, to increase the slump, a better option is maintaining the free w/b ratio at 0.55 by considering the water absorption of CSA.

3.2.2. Temperature

The temperature of fresh concrete is an important parameter to ensure the quality of concrete, as it indicates the hydration rate of cement. In this research, the temperature of the fresh concrete was measured with a digital thermometer according to the ASTM C1064/C1064M-17 standard [5]. Fig. 6 illustrates the temperature of the fresh concrete at the time of mixing. The temperature of the control mix-CSA 0-was 32.7 °C, and all concrete mixes with coconut shell ash- CSA 15, CSA 20, CSA 25 and CSA 30- had lower temperature than CSA 0 mix. In addition, the temperature of concrete mixes at the time of mixing has decreased with increasing the CSA content. Therefore, it is clear that CSA can reduce the temperature of fresh concrete.

There were three reasons to reduce the temperature of concrete mixes with increasing CSA. The first reason was the reduction of cement content. The chemical reaction between cement and water generates heat, raising the concrete temperature [4]. The temperature reduces when reducing the cement content because less cement quantity involves hydration and less heat generation. The second reason was that the CSA has a pozzolanic activity. CSA is a pozzolan, according to Table 3, and it reacts with hydrated cement products. Therefore, heat generation reduced at the time of mixing because of delaying pozzolanic reaction. The third reason was the size of CSA particles. There are more coarse particles in the CSA than in cement, as shown in Fig. 3. Coarse particles take more time for the reaction because of less surface area. Less surface area initially exposes fewer chemical constituents to react with water. Therefore, heat generation reduced at the time of mixing by increasing the CSA.

The temperature of concrete should be less than 35 °C during concrete placing [5]. All concrete mixes with CSA had lower temperature than the control mix in this research. Therefore, all concrete mixtures with CSA- CSA 15, CSA 20, CSA 25 and CSA 30- can be selected based on the temperature.

3.3. Properties of hardened concrete

This section presents and discusses the hardened concrete properties, namely compressive strength, density and water absorption.

3.3.1. Compressive strength

Compressive strength was the most critical parameter for considering the optimal concrete mix designs in this research. Therefore, compressive strength after 7 days, 28 days and 56 days of curing of every mix was measured with nine cubes per mix. Compressive strength tests were performed according to the BS EN 12390-3:2019 [18] using a compression testing machine to verify whether concrete can achieve the target compressive strength after 28 days of curing or not. In this research, the target compressive strength after 28 days of curing was 25 MPa because most structural designs are commonly carried out with this target compressive strength in Sri Lanka [51]. Fig. 7 shows the compressive strength of concrete mixes at the age of 7 days, 28 days and 56 days. The compressive strength of every concrete mix has increased up to 56 days because mainly C_3S ($3CaO.SiO_2$) and C_2S ($2\ CaO.SiO_2$) in the cement react with water to form C-S-H gel. The mix design of the CSA 0 mix was precise because CSA 0 mix achieved the target compressive strength after 28 days of curing, and it was 27.05 MPa.

As shown in Fig. 7, with increasing the CSA content, compressive strength at the age of 28 days has increased up to 15% replacement level (CSA 15) and then compressive strength has decreased. Maximum compressive strength at the age of 28 days was 27.31 MPa, and it is clear that CSA can increase the compressive strength of concrete. Variation of compressive strength at the age of 28 days of concrete can be explained by two characteristics of CSA: filler effect & pozzolanic effect. As discussed in section 3.1.1, CSA has excellent gradation; therefore, it fills the

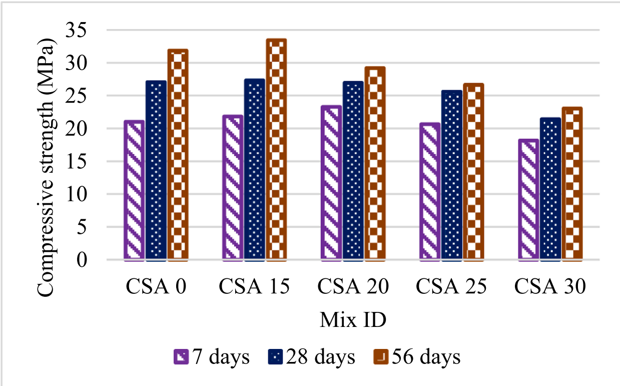

Fig. 7. Compressive strength of concrete mixes after curing.

voids in concrete, known as the filler effect. This filler effect contributed to increasing strength until filling all voids and then contributed to decreasing strength after filling all voids. As discussed in Section 3.1.2, CSA reacts with hydrated products of cement to form C-S-H gel known as pozzolanic effect. This contributes to reduce strength because CSA produces less C-S-H gel compared to the cement. However, the overall impact has positively affected up to the CSA 15 mix at the age of 28 days and 56 days.

Fig. 7 indicates that the filler effect positively impacted the compressive strength of concrete up to 20% replacement (CSA 20) because compressive strength at the age of 7 days has increased up to CSA 20 mix. However, at 28 days and 56 days, CSA 20 mix has less compressive strength than CSA 15 mix because the negative impact of less C-S-H gel formation is higher than the positive impact of the filler effect of CSA. In this research, CSA 15, CSA 20 and CSA 25 could achieve the target compressive strength at 28 days. In addition, these mixes have shown more than 65% of the target compressive strength at the age of 7 days, similar to the control mix. Early strength benefits the construction industry because formwork can be removed early and thus speed up the construction process. Therefore, CSA 15, CSA 20, and CSA 25 mixes are the best mixes based on the compressive strength of concrete.

3.3.2. *Density*

The density of concrete is a significant parameter because it contributes to the self-weight of the structure. In this research, the saturated density of the hardened concrete mixes was measured according to BS EN 12390-7:2019 at the age of 7 days, 28 days, and 56 days [20] using a balance, a ventilated oven, and a water tank. Fig. 8 shows the saturated density of concrete mixes at different curing periods. With the curing, the saturated density of all concrete mixes has increased up to 56 days, because the amount of C-S-H gel increased with the curing period, and C-S-H gel contributed to the increase the weight of concrete.

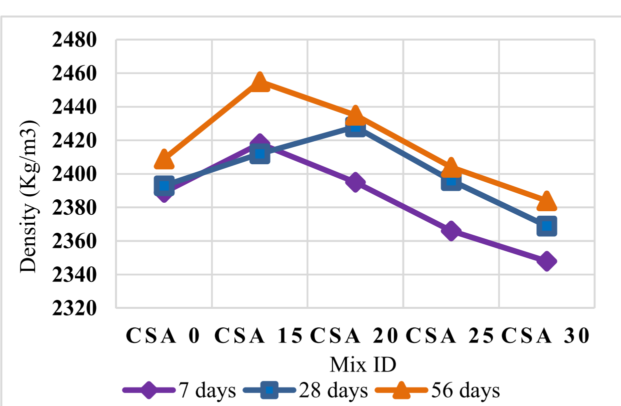

Fig. 8. Saturated density of concrete mixes after curing.

As shown in Fig. 8, with increasing the CSA content, the saturated density of concrete reached the maximum and then it decreased at the age of 7 days, 28 days and 56 days. This finding suggests that CSA affects the saturated density of concrete. As explained in Section 3.1.2, CSA contributes to form less C-S-H gel in concrete. Therefore, when increasing the CSA, the weight of concrete reduces. In addition, as explained in Section 3.1.1, CSA has more carbon particles and absorbs more water. Thus, the weight of concrete increases with increasing the CSA content. Due to the overall impact, concrete density could increase or decrease with the CSA content. At the age of 7 days and 56 days, CSA 15 mix had the maximum saturated density because the weight increment due to the water absorption was higher than the weight decrement due to the C-S-H gel reduction when compared with the CSA 0 mix. However, the saturated density of all concrete mixes with CSA has varied between 2350 Kg/m3 and 2450 Kg/m^3. The saturated density of the CSA 0 mix has also varied around 2400 Kg/m^3. Therefore, all concrete mixes- CSA 15, CSA 20, CSA 25 and CSA 30- can be selected based on saturated density.

3.3.3. *Water absorption*

Water absorption is a good indicator of the durability of concrete. Therefore, the water absorption of concrete mixes was measured as per the BS EN 1097-5: 2008 standard [13] using a balance and a ventilated oven. Fig. 9 shows the water absorption of concrete mixes at different curing periods. Water absorption of every concrete mix reduced as concrete cured. The total voids of concrete can explain this phenomenon, as concrete allows the water to enter concrete's voids. With the curing time, C-S-H gel in concrete mix increased, and total voids decreased.

According to the CSA 0, CSA 20, CSA 25 and CSA 30 mixes, water absorption of concrete mixes increased with increasing CSA content. This phenomenon happened because of increasing the total voids in concrete. CSA has higher carbon particles, and when increasing the CSA, total voids increase. In addition, CSA produces less C-S-H gel than cement, and when the CSA increases, total voids increase. Unexpectedly, CSA 15 mix had higher water absorption. It seems more voids were formed at the outer surface of concrete in this mix. In addition, the reduction of the water absorption from the 7 days to 56 days of the CSA 20, CSA 25, and CSA 30 mixes were 42%, 25% and 12%, respectively. Therefore, it is evident that with increasing the CSA, C-S-H gel formation reduces. In this research, water absorption of the CSA 20 mix was more limited than the CSA 0 mix, and water absorption of the CSA 25 mix was similar to the CSA 0 mix after 28 days and 56 days of curing. Therefore, CSA 20 and CSA 25 mixes are the best mixes based on water absorption.

3.4. *Microstructural properties of concrete*

SEM images of concrete were determined according to the ASTM

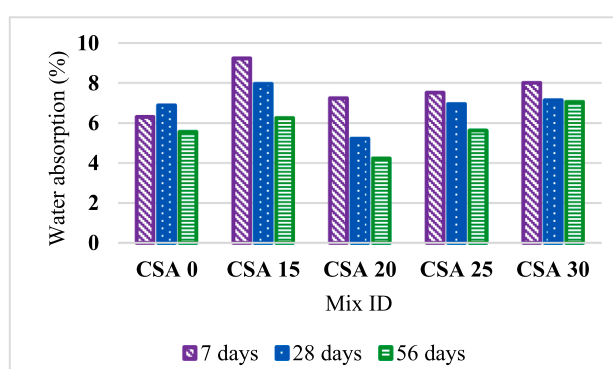

Fig. 9. Variation of the water absorption after curing.

C1723-16 standard at the age of 7 days and 28 days to determine the microstructural properties of concrete [8]. Concrete is a non-conductive material; therefore, a gold coating was applied on the surface of concrete samples to improve the imaging of samples. Fig. 10 shows the micro-structural images of the CSA 0, CSA 20 and CSA 30 mixes at 7 and 28 days. Unreacted cement and CSA particles in concrete were readily observed from the SEM images because the appearance of the cement and CSA particles was observed early, as discussed in Section 3.1.3. In addition, the appearance of the hydration products of cement was observed according to a previous study [25].

Concrete had more calcium hydroxide (CH), C-S-H gel and less unreacted cement or CSA particles at the age of 28 days than at the age of 7 days as shown in Fig. 10. This phenomenon happened because of hydraulic activity of cement and pozzolanic activity of CSA during the curing. Compressive strength of concrete can be increased with the curing period because of the densification of the microstructure. This hypothesis is proved by the compressive strength of concrete mixes, as shown in Fig. 7. According to the SEM images of concrete mixes at the age of 28 days, CSA 20 mix has more C-S-H gel and less Calcium hydroxide (CH) than CSA 0 mix. This phenomenon happened because CSA has pozzolanic activity. In addition, CSA 30 mix has many unreacted CSA particles and less C-S-H gel than the CSA 20 mix because of the

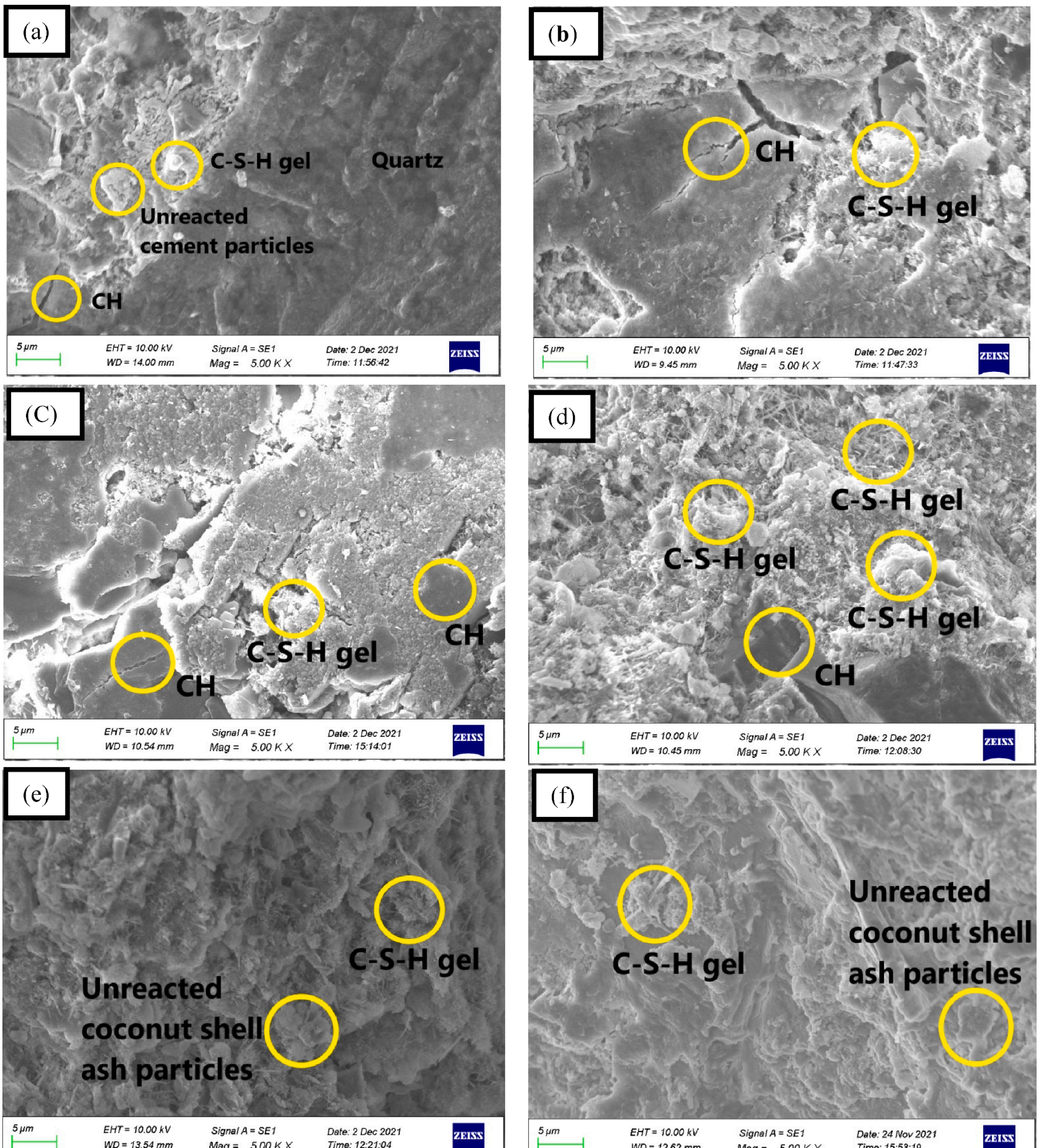

Fig. 10. SEM image of the (a) CSA 0 at 7 days (b) CSA 0 at 28 days (c) CSA 20 at 7 days (d) CSA 20 at 28 days (e) CSA 30 at 7 days (f) CSA 30 at 28 days.

reduction of the cement content. Therefore, it is possible to hypothesise that with increasing the CSA content, the compressive strength increases up to the maximum and then decreases, and it was proved by Fig. 7. As shown in Fig. 10, CSA 30 mixes have more unreacted CSA particles and less C-S-H gel than the other concrete mixes. Therefore, SEM images suggest that CSA 30 mix is not suitable for future designs.

3.5. Environmental impact

This section discusses the environmental impact of five concrete mixes developed in this study.

3.5.1. Environmental impact assessment

A life cycle assessment (LCA) was carried out to evaluate and compare the environmental impact of concrete mixes. In the LCA analysis, life cycle boundaries were clearly defined to ensure the transparency of the results. According to the BS EN15978:2011 [15], a building has five life cycle stages: product stage (A1-A3), construction process stage (A4-A5), use stage (B1-B7), end of life stage (C1-C4), and benefits and loads beyond the boundary stage (D). The product stage has been divided into three processes: raw material supply (A1), transport (A2) and manufacturing (A3). For all concrete mixes, the manufacturing process (A3) was the same, and therefore, raw material supply (A1) and transport (A2) processes were only considered. Seven impact categories-global warming potential (GWP), ozone depletion potential (ODP), acidification potential (AP), eutrophication potential (EP), formation potential of tropospheric ozone (POCP), abiotic depletion potential for non-fossil (ADPE) and fossil resources (ADPF)- were analysed according to the BS EN 15804(2012) + A1(2013) [14].

3.5.2. Functional unit

In this research, the functional unit was the production and delivery of the materials to produce a cubic meter of concrete at the Kurunegala batching plant. Fig. 11 shows the system boundary for LCA.

3.5.3. Data underpinning the study

Various data sources, as shown in Table 4 have been followed to calculate the seven impact categories of concrete mixes. Coconut shells were collected and transported 20 km to burn, grind and sieve. The environmental impact for CSA production was calculated based on the energy consumption data. A muffle furnace with the same burning temperature was selected instead of a diesel incinerator for the calculation. All materials for concrete production were sourced locally.

3.5.4. Environmental impact

Seven environmental impact categories from part of the life cycle were considered in this research. Therefore, the environmental impact

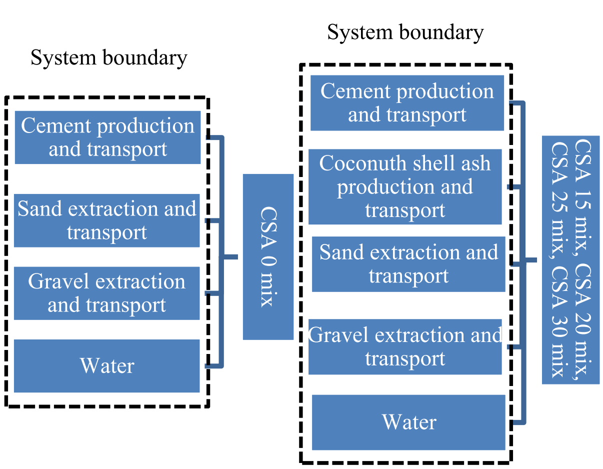

Fig. 11. LCA system boundary for concrete mixes.

of concrete mixes could be compared within this study only. Table 5 presents the potential environmental impact quantities for 1 cubic meter of concrete, considering the production and transport of materials for different mix designs.

The environmental impact of concrete mixes with CSA are lower than the control mix in GWP, AP, POCP and ADPF categories and are higher than the control mix in the ODP, EP and ADPE categories. GWP is the most crucial environmental impact category, and it has the highest weighting factor [49]. Therefore, GWP category was considered to compare and select concrete mixes that have less impact on the environment. Fig. 12 shows the environmental impact reduction in GWP category of concrete mixes in comparison with the control mix. The environmental impact reduces with increasing the CSA content. When considering the CSA 15, CSA 20, CSA 25 and CSA 30 mixes, environmental impact in GWP category reduces over 10%, 15%, 20% and 25% respectively.

3.6. Selection of the optimal concrete mix design

This research was performed to determine the optimal concrete mix with CSA to reduce the potential environmental impact, whilst achieving defined structural performance. As discussed in Section 3.5, GWP is the most crucial environmental impact category, and it reduced with increasing the CSA content of concrete mixes. However, structural performance of concrete varied with the CSA content. Therefore, fresh, hardened, and microstructural properties were also considered to select the optimal concrete mix in this research.

The slump of the fresh concrete mixes was measured at 0 h, 0.5 h and 1 h after mixing. For the normal reinforcement concrete, slump should be higher than 40 mm and only CSA 15 and CSA 20 mixes achieved that requirement. Therefore, they were selected as best mixes based on the slump. The temperature of the fresh concrete mixes was measured at the time of mixing, and the temperature of all mixes was less than 35 ^{0}C. Therefore, CSA 15, CSA 20, CSA 25 and CSA 30 mixes were selected based on the temperature. In this research, compressive strength was the most critical parameter because the target compressive strength of concrete after 28 days of curing was 25 MPa. CSA 15, CSA 20 and CSA 25 mixes were selected as best mixes because they achieved the target compressive strength. The density of concrete mixes varied around 2350–2450 Kg/m^{3,} similar to the control mix. Therefore CSA 15, CSA 20, CSA 25 and CSA 30 mixes were selected based on the density. Water absorption indicates the durability of concrete. At 28 days and 56 days, water absorption of the CSA 20 mix was less than the CSA 0 mix, and water absorption of the CSA 25 mix was similar to the CSA 0. Therefore, CSA 20 and CSA 25 were selected as the best mixes based on the water absorption. According to the SEM images, the microstructural properties of CSA 0, CSA 20 and CSA 30 mixes were investigated at the age of 7 days and 28 days. CSA 30 mix was rejected because of higher unreacted CSA particles and less C-S-H gel.

When considering selected mixes, CSA 15 and CSA 20 mixes were the best mixes according to the fresh concrete properties, and CSA 20 and CSA 25 mixes were the best mixes according to the hardened concrete properties. In addition, except CSA 30 mix, all mixes were proper mixes according to the microstructural properties. CSA 20 mix design was the optimal concrete mix design because it achieved the fresh, hardened and microstructural properties of concrete and reduced the environmental impact over 15% in GWP category.

4. Conclusion

This research was performed to determine the optimal concrete mix CSA to reduce the environmental impact whilst achieving defined structural performance. The target compressive strength of concrete after 28 days of curing was 25 MPa because structural designs are commonly carried out with this target compressive strength in Sri Lanka. Five concrete mixes were produced following Building Research

Table 4
Data source and transport material distances.

Input	Data Source	Geographical Scope	Year	EPD registration no	Travel Distance (km)
Cement	Cement Product (OPC,PPC,PSC,PCC) [54]	India	2022	S-P-05019	100
CSA	Burned, grinded and sieved using hydroelectricity	N/A	N/A	N/A	10
Fine aggregate	Natural inert materials “sand and gravel”- Extracted from artificial quarry [28]	Italy	2020	EPDITALY0088	140
Coarse aggregate	Crushed stone construction aggregate products, Oslo and Baerum [27]	Norway	2018	NEPD-1537–527-EN	20
Energy	Hydroelectricity from Trollheim Power Station [50]	Norway	2019	NEPD-1685–676-EN	N/A
Road transport	GaBi Database: Truck, Bharat stage II, 12–14 t gross weight / 9.3 t payload capacity	India	2021	N/A	N/A

Table 5
Environmental impact of concrete mixes.

Impact category	Unit	CSA 0 mix	CSA 15 mix	CSA 20 mix	CSA 25 mix	CSA 30 mix
GWP	kg CO2 -eq.	3.97E + 02	3.43E + 02	3.25E + 02	3.06E + 02	2.88E + 02
ODP	kg CFC11 -eq	4.67E-07	4.87E-07	4.94E-07	5.01E-07	5.08E-07
AP	kg SO2 -eq	1.42E + 00	1.22E + 00	1.16E + 00	1.09E + 00	1.02E + 00
EP	l kg PO4 3- -eq.	1.83E-02	3.12E-02	3.54E-02	3.97E-02	4.40E-02
POCP	kg C2H4 -eq.	1.04E + 00	8.86E-01	8.33E-01	7.80E-01	7.27E-01
ADPE	kg Sb -eq.	1.59E-05	1.78E-05	1.84E-05	1.91E-05	1.97E-05
ADPF	MJ NCV	2.56E + 03	2.22E + 03	2.11E + 03	2.00E + 03	1.89E + 03

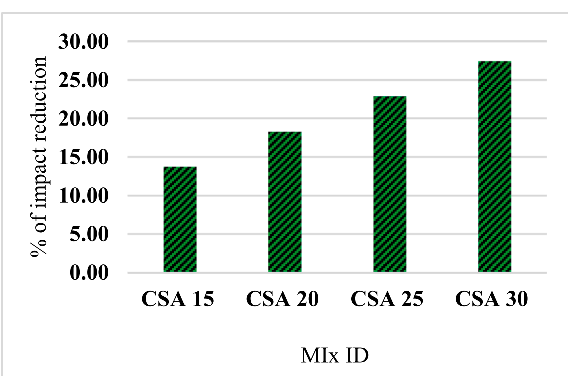

Fig. 12. The percentage of environmental impact reduction in GWP category.

Establishment (BRE) method with CSA replacing cement by 0%, 15%, 20%, 25% and 30%, naming the mixes as CSA 0, CSA 15, CSA 20, CSA 25 and CSA 30 respectively.

The properties of cement and CSA were determined by SEM analysis, EDS analysis, XRF analysis and DIA analysis to explain the performance of concrete with CSA. Fresh, hardened and microstructural properties and the environmental impact of all concrete mixes were observed to select the optimal concrete mix design. In this research, slump and temperature reduced with increasing CSA content. Compressive strength, density and water absorption of concrete mixes increased up to the maximum and then decreased based on the properties of CSA. Microstructural properties were investigated using SEM images, and they showed the unreacted cement and coconut shell particles in addition to the C-S-H gel and $Ca(OH)_2$ in concrete mixes. Environmental impact was analysed under seven categories. GWP is the most crucial environmental impact category and it reduced with increasing the CSA content. Considering the structural performance and environmental impact, CSA 20 mix was selected as the optimal concrete mix, and it reduced the environmental impact in GWP category over 15% in this research. It is recommended that cement can be replaced with CSA by 20% to produce concrete by achieving target compressive strength as 25 MPa.

The followings are significant outcomes in this research:

- CSA has more surface roughness, more carbon particles and better gradation than cement due to the manufacturing process.
- The slump of concrete reduces with increasing the CSA content, and CSA 15 and CSA 20 mixes have sufficient workability for handling.
- The compressive strength increases up to the CSA 15 mix and then decreases with increasing CSA content at the age of 28 days and 56 days.
- Global warming potential (GWP) is the most crucial environmental impact category, and it reduces with increasing the CSA content of concrete mixes.

The limitations of this study have been described below:

This research study was performed within a limited period as a requirement of the MSc Structural Design and Construction Management degree of Kingston University London. This research study developed only five concrete mixes to determine the concrete performance with coconut shell ash due to resource limitations. Experiments used to find the chemical composition of cement and CSA were limited to XRF and EDS because of the unavailability of the instrument used for XRD. Target compressive strength was limited to 25 MPa to find the optimal replacement due to the limited period. This study was conducted with limited resources such as finance and equipment, so only the compressive strength test was performed to assess the overall mechanical strength of concrete. Even though concrete strength increases with time because of CSA, the curing period was limited to 56 days of curing due to the limited period.

5. Future recommendations

The following are some recommendations for future studies:

- Future studies should replace the cement with coconut shell ash for various concrete grades to determine the optimal replacement level for all concrete grades to produce sustainable concrete.
- Future studies should identify other properties in addition to the compressive strength such as tensile strength, flexural strength, and shrinkage of concrete.

CRediT authorship contribution statement

Kavishan Sathsara Ranatunga: Writing – original draft, Methodology, Investigation, Formal analysis. **Enrique del Rey Castillo:** Writing – review & editing, Validation, Supervision, Project administration, Methodology, Conceptualization. **Charlotte Louise Toma:** Writing – review & editing, Validation, Supervision, Methodology, Conceptualization.

Declaration of Competing Interest

The authors declare that they have no known competing financial interests or personal relationships that could have appeared to influence the work reported in this paper.

Data availability

Data will be made available on request.

Acknowledgements

The authors would like to thank the staff of Kingston University library for sharing relevant standards, journal papers and books quickly. The authors would also like to thank the Sri Lankan government institutions and universities for their support to perform the various tests.

Funding

This research did not receive any specific grant from funding agencies in the public, commercia, or not-for-profit sectors.

References

[1] M.A. Adajar, Compressive strength and durability of concrete with coconut shell ash as cement replacement, Int. J. GEOMATE 18 (70) (2020), https://doi.org/10.21660/2020.70.9132.
[2] M. Agarwal, E.R. del Castillo, Normal and controlled low-strength material concrete with high volume of fly ash and glass waste, ACI Mater. J. 119 (4) (2022), https://doi.org/10.14359/51734687.
[3] A.M. Alshamsi, A.R. Sabouni, A.H. Bushlaibi, Influence of set-retarding superplasticisers and microsilica on setting times of pastes at various temperatures, Cem. Concr. Res. 23 (3) (1993) 592–598, https://doi.org/10.1016/0008-8846(93)90009-X.
[4] American Concrete Institute. *Cementitious Materials for Concrete* (2013).
[5] ASTM International, ASTM C1064/C1064M-17: Standard Test Method for Temperature of Freshly Mixed Hydraulic-Cement Concrete, American Society for Testing and Materials, 2017.
[6] ASTM International, ASTM E1508-12a(2019): Standard Guide for Quantitative Analysis by Energy-Dispersive Spectroscopy, American Society for Testing and Materials, 2019.
[7] ASTM International, ASTM E1621-21: Standard Guide for Elemental Analysis by Wavelength Dispersive X-Ray Fluorescence Spectrometry, American Society for Testing and Materials, 2021.
[8] ASTM International, ASTM C1723-16(2022): Standard Guide for Examination of Hardened Concrete Using Scanning Electron Microscopy, American Society for Testing and Materials, 2022.
[9] E. Badogiannis, G. Kakali, G. Dimopoulou, E. Chaniotakis, S. Tsivilis, Metakaolin as a main cement constituent. Exploitation of poor Greek kaolins, Cem. Concr. Compos. 27 (2) (2005) 197–203.
[10] B. Beckhoff, H.B. Kanngießer, N. Langhoff, R. Wedell, H. Wolff (Eds.), Handbook of Practical X-Ray Fluorescence Analysis, Springer Berlin Heidelberg, Berlin, Heidelberg, 2006.
[11] D.P. Bentz, P.E. Stutzman, Evolution of porosity and calcium hydroxide in laboratory concretes containing silica fume, Cem. Concr. Res. 24 (6) (1994) 1044–1050, https://doi.org/10.1016/0008-8846(94)90027-2.
[12] N. Bheel, S.K. Mahro, A. Adesina, Influence of coconut shell ash on workability, mechanical properties, and embodied carbon of concrete, Environ. Sci. Pollut. Res. 28 (5) (2021) 5682–5692, https://doi.org/10.1007/s11356-020-10882-1.
[13] BSI, BS EN 1097-5: 2008 : Tests for Mechanical And Physical Properties of Aggregates Determination of the Water Content by Drying in a Ventilated Oven, British Standards Institution, 2008.
[14] Bsi, BS EN 15804: 2012 +A1: 2013 : Sustainability of Construction Works. Environmental Product Declarations. Core Rules for the Product Category of Construction Products, British Standards Institution, 2012.
[15] BSI, BS EN 15978:2011: Sustainability of Construction Works. Assessment of Environmental Performance of Buildings. Calculation method, British Standards Institution, 2012.
[16] BSI, BS EN 1097-6: 2013 : Tests for mechanical and physical properties of aggregates - Determination of particle density and water absorption, British Standards Institution, 2013.
[17] BSI, BS EN 12350-2: 2019 : Testing fresh concrete - Slump test, British Standards Institution, 2019.
[18] BSI, BS EN 12390-3: 2019 - TC: Testing hardened concrete - Compressive strength of test specimens, British Standards Institution, 2019.
[19] BSI, BS EN 933-2: 2020 : Tests for geometrical properties of aggregates - Determination of particle size distribution. Test sieves, nominal size of apertures, British Standards Institution, 2020.
[20] BSI, BS EN 12390-7: 2019 : Testing hardened concrete - Density of hardened concrete, British Standards Institution, 2020.
[21] W. Bumrongjaroen, et al., Application of glass corrosion tests to the reactivity of fly ash. The World of Coal Ash (WOCA), Kentucky, USA, 2007.
[22] C. Carde, R. François, Modelling the loss of strength and porosity increase due to the leaching of cement pastes, Cem. Concr. Compos. 21 (3) (1999) 181–188, https://doi.org/10.1016/S0958-9465(98)00046-8.
[23] V. Charitha, V.S. Athira, V. Jittin, A. Bahurudeen, P. Nanthagopalan, Use of different agro-waste ashes in concrete for effective upcycling of locally available resources, Constr. Build. Mater. 285 (2021), 122851, https://doi.org/10.1016/j.conbuildmat.2021.122851.
[24] P. Chindaprasirt, C. Jaturapitakkul, T. Sinsiri, Effect of fly ash fineness on microstructure of blended cement paste, Constr. Build. Mater. 21 (7) (2007) 1534–1541, https://doi.org/10.1016/j.conbuildmat.2005.12.024.
[25] S. Diamond, The microstructure of cement paste and concrete—a visual primer, Cem. Concr. Compos. 26 (8) (2004) 919–933, https://doi.org/10.1016/j.cemconcomp.2004.02.028.
[26] Expert Market Research. *Global Cement Market Report and Forecast 2023-2028* (2022).
[27] A.S. Franzefoss Pukk, Crushed Stone Construction Aggregate Products, The Norwegian EPD Foundation, Oslo and Bærum, 2018.
[28] GRUPPO BASSANETTI. *Natural inert materials "Sand and gravel" Extracted from an artificial quarry basin.* EPD Italy (2020).
[29] IPCC, Climate Change 2022: Impacts, Adaptation and Vulnerability, Intergovernmental Panel on Climate Change, 2022.
[30] ISO, ISO 13322-2:2006: Particle size analysis — Image analysis methods — Part 2: Dynamic image analysis methods, International Organization for Standardization, 2006.
[31] M.C.G. Juenger, R. Snellings, S.A. Bernal, Supplementary cementitious materials: New sources, characterization, and performance insights, Cem. Concr. Res. 122 (2019) 257–273.
[32] P. Kara De Maeijer, B. Craeye, R. Snellings, H. Kazemi-Kamyab, M. Loots, K. Janssens, G. Nuyts, Effect of ultra-fine fly ash on concrete performance and durability, Constr. Build. Mater. 263 (2020) 120493.
[33] S.A. Khedr, M.N. Abou-Zeid, Characteristics of silica-fume concrete, J. Mater. Civ. Eng. 6 (3) (1994) 357–375.
[34] P. Kikongi, J. Salvas, R. Gosselin, Curve-fitting regression: improving light element quantification with XRF: Light element quantification improvement with XRF, *X-Ray Spectrom.*, 46(5) (2017) 347–355. Available at: https://doi.org/10.1002/xrs.2760.
[35] S.H. Kosmatka, M.L. Wilson, Design and control of concrete mixtures: the guide to applications, methods, and materials, 15. Aufl. Skokie, Ill, Portland Cement Association (Engineering Bulletin, 1), 2011.
[36] R.R. Kumar, et al., An experimental study on concrete using coconut shell ash and egg shell powder, South Asian J. Eng. Technol. 3 (7) (2017) 151–161.
[37] V. Kumar, P. Sharma, An experimental research on the strength characteristics of concrete with ground nut shell ash, fly ash and coconut shell ashas partial replacement of cement, Int. J. Innov. Technol. Explor. Eng. (IJITEE) 8 (8) (2019) 1405–1409.
[38] A. Lyons, *Materials for Architects and Builders.* 6th edn. Sixth edition. | Abingdon, Oxon : Routledge, (2019): Routledge. Available at: https://doi.org/10.1201/9781351109550.
[39] J.D. Maasakkers, D.J. Varon, A. Elfarsdóttir, J. McKeever, D. Jervis, G. Mahapatra, S. Pandey, A. Lorente, T. Borsdorff, L.R. Foorthuis, B.J. Schuit, P. Tol, T.A. van Kempen, R. van Hees, I. Aben, Using satellites to uncover large methane emissions from landfills, Sci. Adv. 8 (32) (2022).
[40] S.A. Miller, G. Habert, R.J. Myers, J.T. Harvey, Achieving net zero greenhouse gas emissions in the cement industry via value chain mitigation strategies, One Earth 4 (10) (2021) 1398–1411.
[41] National Science Foundation. Transforming Waste in order to transform people's lives (2014).
[42] A. Oner, S. Akyuz, An experimental study on optimum usage of GGBS for the compressive strength of concrete, Cem. Concr. Compos. 29 (6) (2007) 505–514.
[43] A. Oner, S. Akyuz, R. Yildiz, An experimental study on strength development of concrete containing fly ash and optimum usage of fly ash in concrete, Cem. Concr. Res. 35 (6) (2005) 1165–1171.
[44] PCA, Survey of Mineral Admixtures and Blended Cements in Ready-Mixed Concrete, Portland Cement Association, Skokie, Illinois, 2000.
[45] P.J. Potts, M. West, Portable X-ray Fluorescence Spectrometry: Capabilities for in Situ Analysis, Royal Society of Chemistry, 2008.
[46] Z. Qin, C. Ma, Z. Zheng, G. Long, B. Chen, Effects of metakaolin on properties and microstructure of magnesium phosphate cement, Constr. Build. Mater. 234 (2020) 117353.
[47] A.A. Ramezanianpour, H. Bahrami Jovein, Influence of metakaolin as supplementary cementing material on strength and durability of concretes, Constr. Build. Mater. 30 (2012) 470–479.
[48] B.B. Sabir, S. Wild, J. Bai, Metakaolin and calcined clays as pozzolans for concrete: a review, Cem. Concr. Compos. 23 (6) (2001) 441–454.
[49] S. Sala, A.K. Cerutti, R. Pant, Development of a weighting approach for the Environmental Footprint, European Union, 2018.
[50] A.S. Statkraft Energi, Hydroelectricity from Trollheim Power Station, The Norwegian EPD Foundation, 2019.

[51] P.T.R.S. Sugathadasa, M.T.R. Jayasinghe, Cost - effective volume batched mixes for grades C25 and C30, *Engineer: J. Inst. Eng., Sri Lanka*, XXXV I (3) (2003) 13–22.

[52] P. Taylor, et al. *Integrated Materials and Construction Practices for Concrete Pavement: A State-of-the-Practice Manual*. Available at: https://trid.trb.org/view/1918788 (Accessed: 20 November 2022) (2019).

[53] D.C. Teychenne, et al., Design of Normal Concrete Mixes, Building Research Establishment, 1997.

[54] UltraTech Cement Ltd, Cement Product (OPC, PPC, PSC, PCC), EPD International AB, 2022.

[55] U.S. Geological Survey. *Mineral commodity summaries 2022*. Reston, VA: U.S. Geological Survey (2022). Available at: https://doi.org/10.3133/mcs2022.

[56] J.T. Utsev, J.K. Taku, Coconut shell ash as partial replacement of ordinary portland cement in concrete production, Int. J. Sci. Technol. Res. 1 (8) (2012) 86–89.

[57] P. Vasanthi, S. Senthil Selvan, P. Murthi, I. Rajasri Reddy, K. Poongodi, Impact of partial replacement of cement by coconut shell ash and coarse aggregate by coconut shell on mechanical properties of concrete, IOP Conf. Ser.: Mater. Sci. Eng. 981 (3) (2020) 032080.

[58] Q. Wang, D. Wang, H. Chen, The role of fly ash microsphere in the microstructure and macroscopic properties of high-strength concrete, Cem. Concr. Compos. 83 (2017) 125–137.

[59] X.-Y. Wang, H.-S. Lee, Modeling the hydration of concrete incorporating fly ash or slag, Cem. Concr. Res. 40 (7) (2010) 984–996.

[60] P.-M. Zhan, Z.-H. He, Z.-M. Ma, C.-F. Liang, X.-X. Zhang, A.A. Abreham, J.-Y. Shi, Utilization of nano-metakaolin in concrete: A review, J. Build. Eng. 30 (2020) 101259.

[61] H. Zhang, Building Materials in Civil Engineering, Elsevier Science, 2011.